

Near-Forward Stimulated Brillouin Scattering

In stimulated Brillouin scattering¹ (SBS) an incident (pump) light wave is scattered by the electron-density fluctuations associated with an ion-acoustic (sound) wave. This process generates a frequency-upshifted (anti-Stokes) light wave and a frequency-downshifted (Stokes) light wave. For most scattering angles the anti-Stokes wave is driven nonresonantly and can be neglected *a priori*. The resulting instability is referred to as three-wave SBS. However, for near-forward scattering the anti-Stokes wave can be driven near-resonantly and must be retained in the instability analysis. When the role of the anti-Stokes wave is significant, the resulting instability is referred to as four-wave SBS.

In this article the spatiotemporal evolution of near-forward SBS is studied in detail. The conditions under which three- and four-wave SBS occur are quantified, and expressions for the saturation times and steady-state gain exponents are derived for both types of instability.

Governing Equations

SBS is governed by the Maxwell wave equation

$$(\partial_t^2 + \omega_e^2 - c^2 \nabla^2) \mathbf{A}_h = -\omega_e^2 n_l \mathbf{A}_h, \quad (1)$$

together with the sound wave equation

$$(\partial_t^2 - c_s^2 \nabla^2) n_l = \frac{1}{2} c_s^2 \nabla^2 \langle \mathbf{A}_h \cdot \mathbf{A}_h \rangle. \quad (2)$$

The electromagnetic potential $\mathbf{A}_h = (\mathbf{v}_h/c_s)(m_e/m_i)^{1/2}$ is the high-frequency electron velocity divided by a characteristic speed that is of the order of the electron thermal speed, n_l is the low-frequency electron-density variation divided by the equilibrium electron density, ω_e is the electron plasma frequency, c_s is the sound speed, m_e and m_i are the electron and ion masses, respectively, and the brackets $\langle \rangle$ signify that only low-frequency terms are retained. The evolution of the light waves is modified by the nonlinear electron current, which is proportional to $n_l \mathbf{A}_h$, and the sound wave is driven by the pondero-

motive force associated with the light waves, which is proportional to $\nabla \langle \mathbf{A}_h \cdot \mathbf{A}_h \rangle$.

The geometry of near-forward SBS is illustrated in Fig. 72.15. The pump wave propagates in the direction of \mathbf{k}_0 , which defines the z axis. By substituting the Ansätze

$$\begin{aligned} \mathbf{A}_h(t, \mathbf{r}) = & \hat{\mathbf{x}} \{ A_0 + A_+ \exp[i(\mathbf{k}_s \cdot \mathbf{r} - \omega_s t)] \\ & + A_- \exp[-i(\mathbf{k}_s \cdot \mathbf{r} - \omega_s t)] \} \\ & \exp[i(\mathbf{k}_0 \cdot \mathbf{r} - \omega_0 t)] + c.c., \end{aligned} \quad (3)$$

$$n_l(t, \mathbf{r}) = N \exp[i(\mathbf{k}_s \cdot \mathbf{r} - \omega_s t)] + c.c. \quad (4)$$

in Eq. (1), where $\mathbf{k}_s \cdot \mathbf{k}_0 \approx 0$ and $\omega_s = c_s k_s$, and using the envelope and paraxial approximations, one can show that

$$[\partial_z + i(k_s^2/2k_0 - \omega_s/v_0)] A_+ = -i(\omega_e^2/2\omega_0 v_0) N A_0, \quad (5)$$

$$[\partial_z - i(k_s^2/2k_0 + \omega_s/v_0)] A_-^* = i(\omega_e^2/2\omega_0 v_0) N A_0^*, \quad (6)$$

where $v_0 = c^2 k_0/\omega_0$ is the group speed of the pump wave. The time derivatives were omitted from Eqs. (5) and (6) because the time taken for the light waves to cross the plasma is much shorter than the time taken by the sound wave to

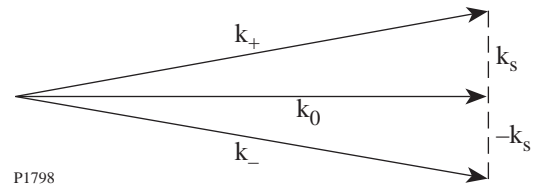


Figure 72.15
Geometry of near-forward SBS. The pump, anti-Stokes, Stokes, and sound waves are denoted by the subscripts 0, +, -, and s, respectively.

respond to the ponderomotive force.² The term $k_s^2/2k_0$ is the reduction in k_z associated with off-axis propagation and the terms $\pm\omega_s/v_0$ are the changes in k_z associated with the anti-Stokes and Stokes frequency shifts, respectively. For all but the smallest angles the latter terms can be neglected. By substituting Ansätze (3) and (4) into Eq. (2), and making the weak-coupling approximation, one can show that

$$\partial_t N = -i(\omega_s/2)(A_0^* A_+ + A_0 A_-^*). \quad (7)$$

By making the substitutions $\omega_0^{1/2} A_+ \rightarrow A_+$, $\omega_0^{1/2} A_-^* \rightarrow A_-$, $\omega_e N/\omega_s^{1/2} \rightarrow N$, and $z/v_0 \rightarrow z$, and adopting the convention that A_0 is real, one can rewrite Eqs. (5)–(7) as

$$(\partial_z \pm i\kappa)A_{\pm} = \mp i\gamma N, \quad (8)$$

$$(\partial_t + \nu)N = -i\gamma(A_+ + A_-) + S(t, x), \quad (9)$$

where

$$\kappa = c^2 k_s^2 / 2\omega_0, \quad \gamma = \omega_e \omega_s A_0 / 2(\omega_0 \omega_s)^{1/2}, \quad (10)$$

ν is a phenomenological term that accounts for the Landau damping of the sound wave, and S is a phenomenological term that maintains the electron-density fluctuations associated with the sound wave at their thermal level in the absence of instability. In addition to the instability described in Eqs. (8) and (9), there is a mirror-image instability, in which the directions of the anti-Stokes and Stokes waves are interchanged, that evolves independently.

Analysis

The Green functions (impulse responses) associated with Eqs. (8) and (9) are defined by the equations

$$(\partial_z \pm i\kappa)G_{\pm} = \mp i\gamma G, \quad (11)$$

$$(\partial_t + \nu)G = -i\gamma(G_+ + G_-) + \delta(t)\delta(z). \quad (12)$$

It follows from Eqs. (11) and (12), and the theory of characteristics, that $G_{\pm}(t, z)$ and $G(t, z)$ can only be nonzero for $t \geq 0$ and $z \geq 0$. The solutions of Eqs. (8) and (9) are

$$A_{\pm}(t, z) = \int_{-\infty}^{\infty} \int_{-\infty}^{\infty} G_{\pm}(t-t', z-z')S(t', z')dt'dz', \quad (13)$$

$$N(t, z) = \int_{-\infty}^{\infty} \int_{-\infty}^{\infty} G(t-t', z-z')S(t', z')dt'dz'. \quad (14)$$

It follows from Eqs. (13) that $G_{\pm}(t-t', z-z')$ describes the effects on the light waves at the point (t, z) of an impulse applied to the sound wave at the point (t', z') . The role of $G(t-t', z-z')$ is similar.

One can solve Eqs. (11) and (12) by using a Laplace transform in time, for which

$$\bar{G}(s, z) = \int_0^{\infty} G(t, z) \exp(-st) dt. \quad (15)$$

The transformed Green functions satisfy the equations

$$(d_z \pm i\kappa)\bar{G}_{\pm} = \mp i\gamma\bar{G}, \quad (16)$$

$$(s + \nu)\bar{G} = -i\gamma(\bar{G}_+ + \bar{G}_-) + \delta(z). \quad (17)$$

By substituting Eq. (17) in Eq. (16) one finds that

$$\frac{d}{dz} \begin{bmatrix} \bar{G}_+ \\ \bar{G}_- \end{bmatrix} = \begin{bmatrix} -\alpha & -\beta \\ \alpha & \beta \end{bmatrix} \begin{bmatrix} \bar{G}_+ \\ \bar{G}_- \end{bmatrix} + \begin{bmatrix} -\mu\delta(z) \\ \mu\delta(z) \end{bmatrix}, \quad (18)$$

where

$$\alpha = \beta + i\kappa, \quad \beta = \gamma^2/(s + \nu), \quad \mu = i\gamma/(s + \nu). \quad (19)$$

If one denotes the eigenvalues of the propagation matrix by $\pm\lambda$, where

$$\lambda = (\alpha^2 - \beta^2)^{1/2}, \quad (20)$$

one can write the solution of Eq. (18) in the form

$$\begin{bmatrix} \bar{G}_+ \\ \bar{G}_- \end{bmatrix} = \begin{bmatrix} -\rho \\ 1 \end{bmatrix} \frac{\mu \exp(\lambda z)}{1 + \rho} - \begin{bmatrix} 1 \\ -\rho \end{bmatrix} \frac{\mu \exp(-\lambda z)}{1 + \rho}, \quad (21)$$

where

$$\rho = \beta/(\lambda + \alpha). \quad (22)$$

It follows from Eqs. (17) and (21) that

$$\bar{G} = -\frac{\mu^2(1-\rho)\exp(\lambda z)}{(1+\rho)} + \frac{\mu^2(1-\rho)\exp(-\lambda z)}{(1+\rho)} + \frac{\delta(z)}{s+\nu}. \quad (23)$$

By using the fact that $(1-\rho)/(1+\rho) = (\alpha-\beta)/\lambda$, one can rewrite the Green functions in the form

$$\bar{G}_{\pm} = \mu[\mp \cosh(\lambda z) + (\alpha-\beta)\sinh(\lambda z)/\lambda], \quad (24)$$

$$\bar{G} = -2\mu^2(\alpha-\beta)\sinh(\lambda z)/\lambda + \delta(z)/(s+\nu). \quad (25)$$

Since the Green functions are even functions of λ , they have no branch points in the complex s plane. The inversion integral associated with the Laplace transform (15) is

$$G(t, z) = \frac{1}{2\pi i} \int_B \bar{G}(s, z) \exp(st) ds, \quad (26)$$

where B denotes the Bromwich contour. To the best of our knowledge, the inversion integrals associated with Eqs. (21) and (23) cannot be done exactly.

1. Three-Wave SBS

The anti-Stokes wave is driven nonresonantly when $\kappa \gg |\beta|$. In this three-wave regime $\lambda \approx \alpha$ and $\rho \approx i\beta/2\kappa$. Since $\text{Re}(\lambda) > 0$ for small s , the $\exp(\lambda z)$ terms in Eqs. (21) and (23) correspond to spatial growth, whereas the $\exp(-\lambda z)$ terms correspond to spatial decay. The growing terms all contain the factor $\exp(i\kappa z)$, which is the spatial dependence required to drive the Stokes response resonantly. The transformed Green functions

$$\bar{G}_+ \approx -\mu[\rho \exp(\alpha z) + \exp(-\alpha z)], \quad (27)$$

$$\bar{G}_- \approx \mu \exp(\alpha z), \quad (28)$$

$$\bar{G} \approx -\mu^2[\exp(\alpha z) - \exp(-\alpha z)] + \delta(z)/(s+\nu). \quad (29)$$

The second terms on the right sides of Eqs. (27) and (29) are required for small values of z but can be neglected for large values of z , as one can verify by evaluating the inversion integrals.

For large values of t one can use the method of steepest descent³ to evaluate the inversion integrals. The Stokes response

$$G_-(t, z) \sim \frac{i\gamma \exp[i\kappa z + 2\gamma(tz)^{1/2} - \nu t]}{2(\gamma\pi)^{1/2}(tz)^{1/4}}, \quad (30)$$

and the anti-Stokes and sound responses

$$G_+(t, z) \sim i(\gamma/2\kappa)(t/z)^{1/2} G_-(t, z), \quad (31)$$

$$G(t, z) \sim -i(t/z)^{1/2} G_-(t, z), \quad (32)$$

respectively. Equations (30) and (32) are the usual results for three-wave SBS, in which the anti-Stokes response is neglected *a priori*.⁴ For future reference, notice that the coefficient of the second term in the exponent of the Stokes response is real: In three-wave SBS the Stokes frequency shift equals the sound frequency. Let

$$t_3 = \gamma^2 z / \nu^2, \quad g_3 = \gamma^2 z / \nu \quad (33)$$

and

$$\tau = \kappa^2 z / \gamma^2. \quad (34)$$

The Stokes and sound responses grow until $t \approx t_3$, at which time their gain exponent is g_3 .^{4,5} Subsequently, they decay in a time that is comparable to the growth time. It is clear from Eq. (31) that as the Stokes and sound responses grow, they produce a weaker anti-Stokes response that grows along with them. At intermediate times $G_+/G_- \sim \gamma/\kappa$. The smallness parameter γ/k , which is the ratio of the temporal growth rate of three-wave SBS to the Stokes frequency shift associated with off-axis propagation, also arises when one studies the temporal growth of near-forward SBS.⁶ When $t \sim \tau$ the amplitudes of the anti-Stokes and Stokes responses are comparable. Since the anti-Stokes process consumes phonons, the anti-Stokes response moderates the growth of SBS significantly at this time and Eqs. (30)–(32) cease to be valid. This assertion is justified mathematically in Appendix A.

2. Four-Wave SBS

The anti-Stokes wave is driven near-resonantly when $\kappa \ll |\beta|$. In this four-wave regime $\lambda \approx (2i\kappa\beta)^{1/2}$ and $\rho \approx 1 - (2i\kappa/\beta)^{1/2}$. Since $\text{Re}(\lambda) > 0$ for small s , the $\exp(\lambda z)$

terms in Eqs. (21) and (23) correspond to spatial growth, whereas the $\exp(-\lambda z)$ terms correspond to spatial decay. The transformed Green functions

$$\bar{G}_{\pm} \approx \mp \mu [\exp(\lambda z) + \exp(-\lambda z)]/2, \quad (35)$$

$$\bar{G} \approx -\mu^2(1-\rho) [\exp(\lambda z) - \exp(-\lambda z)]/2 + \delta(z)/(s+\nu). \quad (36)$$

The second terms on the right sides of Eqs. (35) and (36) are required for small values of z but can be neglected for large values of z , as one can verify by evaluating the inversion integrals.

For large values of t one can use the method of steepest descent to evaluate the inversion integrals. The anti-Stokes and Stokes responses

$$G_{\pm}(t, z) \sim \mp \frac{\gamma e^{i5\pi/12} \exp\left[3e^{i\pi/6}(\gamma^2 \kappa z^2 t/2)^{1/3} - \nu t\right]}{(12\pi)^{1/2} (\gamma^2 \kappa z^2 t/2)^{1/6}}, \quad (37)$$

respectively, and the sound response

$$G(t, z) \sim e^{-i\pi/3} (4\kappa t/\gamma z)^{1/3} G_{-}(t, z). \quad (38)$$

It is clear from Eqs. (37) that the anti-Stokes and Stokes responses are comparable. Let

$$t_4 \approx 3^{3/4} \gamma \kappa^{1/2} z / 4\nu^{3/2}, \quad g_4 \approx 3^{3/4} \gamma \kappa^{1/2} z / 2\nu^{1/2}. \quad (39)$$

The impulse responses grow until $t \approx t_4$, at which time their gain exponent is g_4 .^{5,7} Subsequently, they decay in a time that is comparable to the growth time. When the Stokes response is maximal, the temporal rate of change of its exponent is $i\nu/\sqrt{3}$: In four-wave SBS the Stokes frequency shift differs from the sound frequency by an amount that is proportional to the damping rate of the sound wave. It is verified in Appendix B that Eqs. (37) and (38) are valid for $t \gg \tau$.

3. Evolution of the Impulse Responses

The spatiotemporal evolution of the impulse responses depends on the parameter $\kappa\nu/\gamma^2$.⁵ Suppose that $\kappa\nu/\gamma^2 \gg 1$; then $t_3 \ll \tau \ll t_4$. It follows from the first of these inequalities that the impulse responses grow and decay according to the three-wave equations [Eqs. (30)–(32)]. Their maximal gain

exponent is g_3 and the four-wave equations [Eqs. (37) and (38)] are never relevant. Conversely, suppose that $\kappa\nu/\gamma^2 \ll 1$; then $\tau \ll t_4 \ll t_3$. It follows from these inequalities that the impulse responses begin to grow according to the three-wave equations, then continue to grow and decay according to the four-wave equations. Their maximal gain exponent is g_4 . Consistent with the assertion that the anti-Stokes response moderates the growth of near-forward SBS, in this parameter regime g_4 is smaller than g_3 by a factor of $(\gamma^2/\kappa\nu)^{1/2}$. Notice that the transition from three-wave to four-wave growth always occurs in the absence of damping.

Discussion

The anti-Stokes and Stokes waves evolve according to Eqs. (13). The properties of the Green functions were discussed in the previous section. To complete our analysis we make the common assumption that the source term is a random function with the statistical properties

$$\langle S(t', z') \rangle = 0, \quad (40)$$

$$\langle S(t', z') S^*(t'', z'') \rangle = \sigma \delta(t' - t'') \delta(z' - z''), \quad (41)$$

where $\langle \rangle$ now denotes an ensemble average.^{8–10} The source strength σ is determined by the requirement that the density fluctuations associated with the sound wave have their thermal values in the absence of instability.^{8–10} It follows from Eqs. (13) and (41) that

$$\langle |A_{\pm}(t, z)|^2 \rangle = \sigma \int_0^z \int_0^t |G_{\pm}(t-t', z-z')|^2 dt' dz'. \quad (42)$$

Because the integrands in Eqs. (42) are non-negative, the contributions to the wave intensities from each source point increase monotonically and saturate in times that are comparable to the Green-function growth times described in the **Analysis** section. The Green-function gain exponents and growth times are proportional to $z - z'$ in both the three-wave and four-wave regimes. Thus, the contributions from adjacent source points ($z' \approx z$) are small and saturate quickly, whereas the contributions from distant source points ($z' \approx 0$) are large and saturate slowly: The saturation times and asymptotic values of the integrals in Eqs. (42) are dominated by the contributions from distant source points.

Suppose that $\kappa\nu/\gamma^2 \gg 1$; then the saturation time $t_s \sim t_3$.¹¹ One can evaluate the integrals in Eqs. (42) by using the method

of steepest descent.³ In steady state the Stokes intensity has the form

$$\langle |A_-(z)|^2 \rangle \sim \frac{\sigma \exp(2g_3)}{4\pi^{1/2} (2g_3)^{1/2}}. \quad (43)$$

Consistent with the discussion of the previous paragraph, the gain exponent for the Stokes intensity is $2g_3$. Equation (43) is the analog for near-forward SBS of the result of Boyd *et al.*⁸ for backward SBS. Conversely, suppose that $\kappa\nu/\gamma^2 \ll 1$; then the saturation time $t_s \sim t_4$.¹¹ In steady state the Stokes intensity has the form

$$\langle |A_-(z)|^2 \rangle \sim \frac{(\gamma^2/\kappa\nu)^{1/2} \sigma \exp(2g_4)}{2^{5/2} 3^{3/4} \pi^{1/2} (2g_4)^{1/2}}. \quad (44)$$

Consistent with the discussion of the previous paragraph, the gain exponent for the Stokes intensity is $2g_4$.

The preceding analysis is based on the weak-coupling approximation, which is not valid for short times, very small scattering angles, or very high pump intensities. A general analysis of Eqs. (1) and (2), which allows the coupling to be strong or weak, is described in Appendix C. When $\kappa\omega_s/\gamma^2 \gg 1$, SBS begins to grow as a strongly coupled three-wave instability, then continues to grow as a weakly coupled three-wave instability.⁵ The preceding results describe the later growth phase. In particular, the value of $\kappa\nu/\gamma^2$ determines whether SBS saturates as a weakly coupled three- or four-wave instability. When $\kappa\omega_s/\gamma^2 \ll 1$, SBS begins to grow as a strongly coupled three-wave instability, then continues to grow as a strongly coupled four-wave instability and saturates as a weakly coupled four-wave instability.⁵ The preceding four-wave results describe the saturation of SBS.

The transient (spatiotemporal) phase of SBS was observed recently by Lal *et al.*¹² In their experiment SBS was initiated by optical mixing rather than density fluctuations associated with the sound wave. There is good agreement between the theoretical predictions described herein, modified to include the effects of a low-intensity probe wave, and the experimental results.

Summary

The spatiotemporal evolution of near-forward SBS was studied in detail. Two types of instability can occur. In three-wave SBS only the Stokes and sound waves interact strongly

with each other and the pump wave. However, as the Stokes and sound waves grow, they produce a weaker anti-Stokes wave that grows along with them. In four-wave SBS the anti-Stokes, Stokes, and sound waves all interact strongly with each other and the pump wave. In the weak-coupling regime the spatiotemporal evolution of SBS depends on the scattering angle through the parameter of $\kappa\nu/\gamma^2$, where γ is the temporal growth rate of three-wave SBS in an infinite plasma, κ is the frequency shift associated with off-axis propagation, and ν is the damping rate of the sound wave. For large scattering angles ($\kappa\nu/\gamma^2 \gg 1$) the instability grows and saturates according to the three-wave equations. The saturation time and steady-state gain exponent are given by Eqs. (33). For small scattering angles ($\kappa\nu/\gamma^2 \ll 1$) the instability begins to grow according to the three-wave equations, then continues to grow and saturates according to the four-wave equations. The saturation time and steady-state gain exponent are given by Eqs. (39). Since the anti-Stokes process consumes phonons, the presence of a strong anti-Stokes wave reduces the saturation time and steady-state gain exponent significantly. The initial growth of SBS in the strong-coupling regime and the subsequent transition to the weak-coupling regime were also discussed briefly.

ACKNOWLEDGMENT

This work was supported by the National Science Foundation under Contract No. PHY-9057093, the U.S. Department of Energy Office of Inertial Confinement Fusion under Cooperative Agreement No. DE-FC03-92SF19460, the University of Rochester, and the New York State Energy Research and Development Authority. The support of DOE does not constitute an endorsement by DOE of the views expressed in this article.

Appendix A: Three-Wave SBS

In the three-wave regime the transformed Green functions can be approximated by Eqs. (27)–(29). The inverse transform of each term in these equations is tabulated,¹³ so it is not difficult to show that

$$G_+(t, z) \approx -\gamma \left\{ (\gamma/2\kappa) (t/z)^{1/2} I_1 \left[2\gamma(tz)^{1/2} \right] \exp(i\kappa z - \nu t) + iJ_0 \left[2\gamma(tz)^{1/2} \right] \exp(-i\kappa z - \nu t) \right\} H(t) H(z), \quad (A1)$$

$$G_-(t, z) \approx i\gamma I_0 \left[2\gamma(tz)^{1/2} \right] \exp(i\kappa z - \nu t) H(t) H(z), \quad (A2)$$

$$G(t, z) \approx \gamma (t/z)^{1/2} I_1 \left[2\gamma(tz)^{1/2} \right] \exp(i\kappa z - \nu t) H(t) H(z) + H(t) \delta(z) \exp(-\nu t). \quad (A3)$$

Equations (30)–(32) follow from Eqs. (A1)–(A3) and the fact that $I_n(x) \sim \exp(x)/(2\pi x)^{1/2}$ as $x \rightarrow \infty$.

One can also derive Eqs. (30)–(32) by using the method of steepest descent. The arguments of the inversion integrals all contain the factor $\exp[\phi(s)]$, where $\phi(s) = \gamma^2 z/(s + v) + st$. The argument function ϕ is maximal at $s = -v + \gamma(z/t)^{1/2}$. At this point $\beta = \gamma(t/z)^{1/2}$ and the three-wave condition $\kappa \gg |\beta|$ is equivalent to the condition $t \ll \kappa^2 z/\gamma^2$, as asserted in the text.

Appendix B: Four-Wave SBS

Equations (37) and (38) were derived by using the method of steepest descent. The arguments of the inversion integrals all contain the factor $\exp[\phi(s)]$, where $\phi(s) = e^{i\pi/4} \gamma z (2\kappa)^{1/2} / (s + v)^{1/2} + st$. The real part of the argument function ϕ is maximal at $s = -v + e^{i\pi/6} (\gamma^2 \kappa z^2 / 2t^2)^{1/3}$. At this point $|\beta| = (2\gamma^4 t^2 / \kappa z^2)^{1/3}$ and the four-wave condition $\kappa \ll |\beta|$ is equivalent to the condition $t \gg \kappa^2 z/\gamma^2$, as asserted in the text.

It was stated in the text that the Stokes frequency shift differs from the sound frequency. One can explain this difference by analyzing four-wave SBS in the frequency domain. Let $s \rightarrow -i\omega$; then the spatial growth rate is $\gamma \kappa^{1/2} [2i/(v - i\omega)]^{1/2}$. It is not difficult to show that the square of the real part of the spatial growth rate is $\gamma^2 \kappa \left[-\omega + (v^2 + \omega^2)^{1/2} \right] / (v^2 + \omega^2)$. The maximal value of the spatial growth rate is $3^{3/4} \gamma \kappa^{1/2} / v^{1/2}$, which corresponds to $\omega = -v/\sqrt{3}$. Thus, the instability selects the Stokes frequency that corresponds to maximal growth.

Appendix C: Strongly Coupled SBS

By substituting the Ansätze

$$\mathbf{A}_h(t, \mathbf{r}) = \hat{\mathbf{x}} \{ A_0 + A_+ \exp(i\mathbf{k}_s \cdot \mathbf{r}) + A_- \exp(-i\mathbf{k}_s \cdot \mathbf{r}) \} \exp[i(\mathbf{k}_0 \cdot \mathbf{r} - \omega_0 t)] + c.c. \quad (C1)$$

$$n_l(t, \mathbf{r}) = n \exp(i\mathbf{k}_s \cdot \mathbf{r}) + c.c. \quad (C2)$$

in Eqs. (1) and (2), using the envelope and paraxial approximations, and making the substitutions $\omega_0^{1/2} A_+ \rightarrow A_+$, $\omega_0^{1/2} A_- \rightarrow A_-$, $\omega_e n / \omega_s^{1/2} \rightarrow n$, and $z/v_0 \rightarrow z$, one can show that

$$(\partial_z \pm i\kappa) A_{\pm} = \mp i\gamma n, \quad (C3)$$

$$\left(\partial_t^2 + 2v\partial_t + \omega^2 \right) n = -2\omega\gamma(A_+ + A_-), \quad (C4)$$

where v is a phenomenological damping term. For simplicity of notation the subscript s was omitted from the sound frequency ω . Equations (C3) and (C4) govern near-forward SBS in the strong-coupling regime and reduce to Eqs. (8) and (9) in the weak-coupling regime.

One can determine the Green functions associated with Eqs. (C3) and (C4) by using a Laplace transform in time. The expressions for the transformed Green functions contain the terms $\exp(\pm\lambda z)$, where $\lambda = (\alpha^2 - \beta^2)^{1/2}$ and $\beta = -2i\omega\gamma^2 / (s^2 + 2vs + \omega^2)$. In the strong-coupling regime $|s| \gg \omega$ and $\beta \approx -2i\omega\gamma^2 / s^2$.

The anti-Stokes wave is driven nonresonantly when $\kappa \gg \beta$. In this three-wave regime $\lambda \approx i\kappa - 2i\omega\gamma^2 / s^2$. The arguments of the inversion integrals contain the factors $\exp[\phi_{\pm}(s)]$, where $\phi_{\pm}(s) = -2i\omega\gamma^2 z / s^2 + st$. The real parts of argument functions ϕ_{\pm} attain their maximal value $3^{3/2} (\gamma^2 \omega z t^2)^{1/3} / 2^{4/3}$ at $s = e^{\mp i\pi/6} (4\gamma^2 \omega z / t)^{1/3}$.⁵ These results are the analogs for near-forward SBS of the results of Mounaix and Pesme,¹⁴ and Hinkel *et al.*,¹⁵ for backward SBS. The three-wave condition $\kappa \gg \beta$ is equivalent to the condition $t \ll \kappa^{3/2} z / \gamma \omega^{1/2}$ and the strong-coupling condition $|s| \gg \omega$ is equivalent to the condition $t \ll \gamma^2 z / \omega^2$.

The anti-Stokes wave is driven near-resonantly when $\kappa \ll \beta$. In this four-wave regime $\lambda \approx 2(\kappa\omega)^{1/2} \gamma / s$ and $\phi(s) = 2(\kappa\omega)^{1/2} \gamma z / s + st$. The argument function attains its maximal value $2^{3/2} (\kappa\omega)^{1/4} (\gamma z t)^{1/2}$ at $s = (\kappa\omega)^{1/4} (2\gamma z / t)^{1/2}$.⁵ Notice that four-wave SBS is a purely growing instability. The four-wave condition $\kappa \ll \beta$ is equivalent to the condition $t \gg \kappa^{3/2} z / \gamma \omega^{1/2}$, which is consistent with the analysis of the preceding paragraph, and the strong-coupling condition is equivalent to the condition $t \ll \gamma \kappa^{1/2} z / \omega^{3/2}$.

The spatiotemporal evolution of SBS in the strong-coupling regime is controlled by the parameter $\kappa\omega/\gamma^2$.⁵ When $\kappa\omega/\gamma^2 \gg 1$, the transition from strong to weak coupling occurs before the transition from strongly coupled three-wave growth to strongly coupled four-wave growth. Thus, SBS begins to grow as a strongly coupled three-wave instability, then continues to grow as a weakly coupled three-wave instability. Subsequently, SBS evolves in the manner described in the **Analysis** section. When $\kappa\omega/\gamma^2 \ll 1$, the transition from strongly coupled three-wave growth to strongly coupled four-wave growth occurs before the transition from strong to weak coupling. This

second transition does not occur until $t \gg \tau$ [Eq. (34)]. Thus, SBS begins to grow as a strongly coupled three-wave instability, then continues to grow as a strongly coupled four-wave instability and saturates as a weakly coupled four-wave instability.

REFERENCES

1. W. L. Kruer, *The Physics of Laser Plasma Interactions*, Frontiers in Physics, Vol. 73 (Addison-Wesley, Redwood City, CA, 1988).
2. One can resolve the propagation of the light waves by using the retarded-time variable $t - z/v_0$ instead of the time variable t . Equations (5)–(7) are unchanged.
3. C. M. Bender and S. A. Orszag, *Advanced Mathematical Methods for Scientists and Engineers* (McGraw-Hill, New York, 1978).
4. R. E. Giacone, C. J. McKinstrie, and R. Betti, *Phys. Plasmas* **2**, 4596 (1995) and references therein.
5. J. S. Li and C. J. McKinstrie, *Bull. Am. Phys. Soc.* **40**, 1722 (1995).
6. C. J. McKinstrie and M. V. Goldman, *J. Opt. Soc. Am.* **B 9**, 1778 (1992).
7. H. A. Rose, D. F. DuBois, and D. Russell, *Sov. J. Plasma Phys.* **16**, 537 (1990).
8. R. W. Boyd, K. Rzazewski, and P. Narum, *Phys. Rev. A* **42**, 5514 (1990).
9. E. A. Williams and R. R. McGowan, in *Research Trends in Physics: Inertial Confinement Fusion*, edited by K. A. Brueckner (American Institute of Physics, New York, 1992), pp. 325–330.
10. P. Mounaix *et al.*, *Phys. Fluids B* **5**, 3304 (1993).
11. In both the three-wave and four-wave regimes, the Green-function growth times are proportional to z . Their temporal widths, which determine the delays between the growth times and the saturation times, are proportional to $z^{1/2}$. Although these delays are increasing functions of z , the ratios of these delays to the growth times, which define the instability time scales, are decreasing functions of z . Thus, the saturation times are asymptotic to t_3 and t_4 .
12. A. K. Lal, K. A. Marsh, C. E. Clayton, C. Joshi, C. J. McKinstrie, J. S. Li, and T. W. Johnston, *Phys. Rev. Lett.* **78**, 670 (1997).
13. M. Abramowitz and I. A. Stegun, ed. *Handbook of Mathematical Functions with Formulas, Graphs, and Mathematical Tables*, Applied Mathematics Series 55 (U.S. Government Printing Office, Washington, DC, 1964).
14. P. Mounaix and D. Pesme, *Phys. Plasmas* **1**, 2579 (1994).
15. D. E. Hinkel, E. A. Williams, and R. L. Berger, *Phys. Plasmas* **1**, 2987 (1994).